



# Effect of combining rules on modeling of asphaltene precipitation

Neda Hajizadeh<sup>1</sup> · Gholamreza Moradi<sup>1</sup> · Siavash Ashoori<sup>2</sup>

Received: 22 July 2020 / Accepted: 18 December 2020 / Published online: 5 February 2021  
© Institute of Chemistry, Slovak Academy of Sciences 2021

## Abstract

Asphaltene deposition causes serious problems in the oil industry and reduces oil recovery. Deposition happens as a consequence of asphaltene precipitation which is a process as a result of a change in thermodynamic stability. Thus, prediction and preventing of the precipitation condition are the first step of preventing asphaltene precipitation and deposition. In this study, a thermodynamic model for asphaltene precipitation has been developed using Peng–Robinson (PR), Soave–Redlich–Kwong (SRK), and a new modification on SRK [modified-SRK equations of state (EOS)]. To modify EOS for non-pure sample (oil sample), van der Waals mixing rule with three types of combining rule containing conventional, Margules, and van Laar type was used. In addition, to verify the derived model, the experiments were conducted on a live oil sample to investigate the effect of pressure reduction and gas injection [nitrogen (0.1, 0.2, and 0.4 mol fraction) and first stage gas (0.2, 0.4 and 0.6 mol fraction)] on asphaltene precipitation. The results show that at low pressures (pressures below 5000 psia), nitrogen is not soluble in oil and the injection of nitrogen reduces asphaltene precipitation because of the liberation of the light component from crude oil; however, increasing the pressure (pressures above 6000 psia) increases the solubility of nitrogen and increases the asphaltene precipitation. For the first stage gas injection, asphaltene precipitation increases because of its high solubility in crude oil at any pressure. The amount of asphaltene precipitation due to first stage gas injection is higher than nitrogen injection except at nitrogen concentration and pressures near the bubble point (pressure of 7000 psia and nitrogen injection of 0.1 mol fraction). According to the modeling results, van Laar type combining rule in conjugated with modified-SRK-EOS predicts the amount of asphaltene precipitation very well at all situations of pressures and different gas injections, and has the least deviation from experimental data rather than the other two types of combining rules; and using mentioned combining formula, the RMSE value decreases to about 50% of the conventional combining rule. It is because of the accurate and distinct interaction parameters of each pair of components in van Laar equation.

**Keywords** Asphaltene precipitation · Equation of state · Combining rule · Gas injection

## List of symbols

APCI	Atmospheric pressure chemical ionization
$a$	Attractive-energy parameter of EOS
$a^{\text{mixture}}$	Attractive-energy parameter of EOS for mixtures
$a_i$	Attractive-energy parameter of component “ $i$ ”
$a_{ij}$	Cross term of parameter “ $a$ ” for pair of components “ $i$ ” and “ $j$ ”
$b$	Co-volume parameter of EOS
$b^{\text{mixture}}$	Co-volume parameter of EOS for mixtures

$\alpha, \psi, \Omega$	EOS parameters
$\Omega$	Acentric factor
Cal.data <sub><math>i</math></sub>	Calculated parameter with a model at Exp. data <sub><math>i</math></sub> condition
Exp.data <sub><math>i</math></sub>	$i$ th experimental data
EOS	Equation/s of state
FCS	Fluorescence correlation spectroscopy
FDPI	Fluorescence depolarization field ionization
FI	Field ionization
FT-ICR	Fourier transform ion cyclotron resonance
$f_i^{\text{oil}}$	Fugacity of asphaltene in residue oil
$f_{\text{As}}^{\text{pure}}$	Fugacity of precipitated asphaltene
$f_i$	Fugacity of component “ $i$ ” in reservoir oil
$f_i^{\text{gas}}$	Fugacity of component “ $i$ ” in gas phase
$f_i^{\text{oil}}$	Fugacity of component “ $i$ ” in residue oil
$f_i^{\text{pure}}$	Fugacity of component “ $i$ ” in pure state
$K_{ij}$	Interaction parameter of component “ $i$ ” with “ $j$ ”

✉ Gholamreza Moradi  
gmoradi@razi.ac.ir

<sup>1</sup> Faculty of Chemical and Petroleum Engineering, Catalyst Research Center, Razi University, Kermanshah, Iran

<sup>2</sup> Department of Petroleum Engineering, Petroleum University of Technology (PUT), Ahvaz, Iran

GOR	Gas oil ratio
GPC	Gel permeation chromatography
LD	Laser desorption
LDI	Laser desorption ionization
LOP	Lower onset pressure
MS	Mass spectroscopy
MW	Molecular weight
$N$	Number of experimental data
$P$	Pressure
$P_b$	Bubble point pressure
$P_c$	Critical pressure
PR	Peng–Robinson
$P_R$	Reservoir pressure
$P_r$	Reduced pressure
$R$	Universal gas constant
RMSE	Root-mean-square error
SALDI	Surface-assisted laser desorption/ionization
SEC	Size exclusion chromatography
SRK	Soave–Redlich–Kwong
$T$	Temperature
$T_c$	Critical temperature
$T_R$	Reservoir temperature
$T_r$	Reduced temperature
$\theta_1, \theta_2, \theta_3$	Adjustable parameters of $K_{ij}$ for PR-EOS
$\xi, \delta$	Parameters of $K_{ij}$ for SRK-EOS
TR-FD	Time-resolved fluorescence depolarization
UOP	Upper onset pressure
wt%	Weight percent
$x_{As}$	Mole fraction of asphaltene in residue oil
$x_i$	Mole fraction of component “ $i$ ” in residue oil
$y_i$	Mole fraction of component “ $i$ ” in gas phase
$y_i^b$	Mole fraction of component “ $i$ ” in gas phase at bubble point pressure
$Z_i$	Mole fraction of component “ $i$ ” in reservoir oil

## Introduction

The oil industry deals with the problem of asphaltene precipitation and deposition such as reduction of the rock permeability and oil recovery (because they change wettability and cause extra pressure drop as a result of blockage mechanisms in wellbore tubing), decrease in flow diffusivity, and fouling problems during transportation and production (Zendehboudi et al. 2013; Hemmati-Sarapardeh et al. 2013; Ahmadi 2012).

Asphaltene is the heaviest and the most polar fraction of petroleum that is the most complicated fraction which alone contains more than 100,000 different molecules (Rastgoo and Kharrat 2017; Hemmati-Sarapardeh et al. 2013; Shirani et al. 2012; Mohammadi and Richon 2007). Asphaltene is insoluble in some substances such as paraffin, but soluble in others such as aromatic compounds (e.g., benzene,

toluene, and pyridine). The chemical structure of asphaltene includes pre-condensed aromatic rings and aliphatic chains (as the main constituent of asphaltene molecules), which results in a broad range of asphaltene molecular weight (Zendehboudi et al. 2013; Hemmati-Sarapardeh et al. 2013; Bouhadda et al. 2007; Duda and Lira-Galeana 2006; Orangi et al. 2006; Buenrostro-Gonzalez et al. 2004); on the other hand, aggregation of asphaltene can cause molecules with a molecular weight range of  $10^3$ – $10^5$  (Rastgoo and Kharrat 2017). Therefore, there has been a wide argument on the molecular weight of asphaltenes. There are many reviews and experimental work on asphaltene molecular weight which are presented in Appendix 1. Asphaltene molecular weight from most of the different experimental method is between 500 and 1000 (g/mol). However, the more probable value that reported by Mullins et al. (2012) is around 750 g/mol (Soleymanzadeh et al. 2018).

Several scientists have reported various theoretical and practical aspects of asphaltene precipitation and deposition. Asphaltene solubility is a function of reservoir thermodynamic conditions, fluid composition, and the properties of the injected fluids. Any variation in temperature, pressure, and composition of the oil that generated as a result of natural pressure depletion, acid stimulation, gas-lift operations, and enhanced oil recovery processes (such as microbial EOR and flooding of incompatible fluids in oil reservoirs) may affect asphaltene precipitate out of the solution (Zendehboudi et al. 2013; Rastgoo and Kharrat 2017; Hemmati-Sarapardeh et al. 2013); whereas deposition can be caused by the formation and growth of a precipitated asphaltene layer on a surface. Therefore, a necessary condition for deposition is the precipitation of asphaltene from liquid solution (Rastgoo and Kharrat 2017).

Controlling heavy organic precipitation through using the solvent treatment, dispersant injection, and mechanical methods are examples of preventing activities for asphaltene precipitation and consequently deposition control. Due to high cost of these techniques and also production loss (as a consequence of asphaltene precipitation and deposition), recognition and prediction of these unwanted phenomena are necessary for design and applying of any EOR technologies. Thus, various experimental works and analytical models introduced in the literature, but a comprehensive approach is still lacking (Zendehboudi et al. 2013; Ahmadi 2012; Abedini and Abedini 2011; Ashoori et al. 2010).

Although experimentally determination of asphaltene precipitation is valuable, they are usually costly and time-consuming. Therefore, an attempt to find an accurate and quick modeling approach is unavoidable (Hemmati-Sarapardeh et al. 2013). In other words, introducing an accurate model for asphaltene precipitation that can be implemented in any reservoir simulator software and provides enough accuracy and performance over the existing methods is very

important. Many researchers applied theoretical models to predict precipitation of heavy organic precipitation, but due to the fuzzy nature of asphaltene molecules and various factors affecting these phenomena, a comprehensive model not introduced yet.

Consideration of asphaltene chemistry plays an essential role in the selection of suitable precipitation model (Zendehboudi et al. 2013). Some authors considered the precipitated asphaltene as solid phase such as Gupta and Thomas et al. (Subramanian et al. 2016; Thomas et al. 1992), and some others considered the precipitated asphaltene as liquid such as Sabbagh et al. (2006). Generally, developed models include three main groups:

- (a) The first group is molecular thermodynamic models in which assume that a real solution created as a result of asphaltene dissolving in crude oil. The validity of this approach depends on asphaltene precipitation reversibility (Zendehboudi et al. 2013; Peramanu et al. 2001).
- (b) The second group is colloidal models which assume the suspension of asphaltene covered by resin in crude oil. Based on this approach, when the resin layer is removed, flocculation and aggregation of asphaltene particles start which result in asphaltene deposition. These models consider precipitation as an irreversible process; therefore, reversibility tests do not support this type of modeling approach (Rastgoo and Kharrat 2017; Zendehboudi et al. 2013).
- (c) The third group is models based on the scaling equation in which the complex properties of asphaltene are not considered. The three variables involved in the scaling equation are the weight percent of precipitated asphaltene (based on the weight of feed oil), the dilution ratio (defined as the ratio of injected solvent volume to weight of crude oil), and the molecular weight of solvent (Zendehboudi et al. 2013; Ahmadi 2012).

As presented in our previous works for our oil sample, experimental data show that precipitation of asphaltene is nearly reversible with a little hysteresis in non-porous media and completely reversible in porous media (Ashoori and Balavi 2014; Abedini et al. 2011). Thus here, asphaltene precipitation is known as a reversible process. By assuming asphaltene precipitation as a reversible process, thermodynamic models and consequently EOS are known as a powerful tool for describing the thermodynamic properties. Many researchers have used equations of state for modeling asphaltene precipitation (Zendehboudi et al. 2013; Pazuki et al. 2007).

Generally, EOS is used for pure fluids. Since oil samples are not known as pure fluids, for modifying available EOS for prediction of asphaltene precipitation, mixing and combining rules are used to extend the use of EOS for mixtures.

In this study, the experimental data of the amount of asphaltene precipitation, during  $N_2$  and first stage gas injection on live oil samples, are generated by the gravimetric method. In addition, a new equation for b-parameter of SRK-EOS is derived that improves the results of EOS modeling of asphaltene precipitation. Finally, the combination of three types of EOS [PR, SRK, and modified-SRK-EOS (Hajizadeh et al. 2020)] with van der Waals mixing rule and three types of combining rule (conventional, Margules, and van Laar type) were used for modeling the precipitation process during gas injection. It is noticeable that conventional type combining rule commonly used by authors and here the last two (i.e., Margules and van Laar type) are used as a novelty work for asphaltene precipitation modeling. The results of the modified-SRK-EOS (Hajizadeh et al. 2020) with van Laar type combining rule showed good matching with experimental data.

## Model description

Generally, equations of state are powerful tools in chemical engineering practice, since they can be used to correlate and (or) predict the thermodynamic properties and phase behavior of pure fluids over large ranges of temperature and pressure. In the literature, there are different studies and reports on applying well-known equations of state for thermodynamic modeling of the asphaltene precipitation process. In this study, different equations of state with Margules and van Laar type of combining rule were used for modeling asphaltene precipitation during natural depletion and gas injection (first stage gas and  $N_2$  gas as injection gas) in a live oil sample. To the best of our knowledge, these types of combining rules have never been used before for modeling asphaltene precipitation.

The following assumptions were used in this study to model asphaltene precipitation.

1. Asphaltene is known as a pseudo-component that is soluble in oil, and its precipitation is known as a reversible process.
2. A component “*i*” precipitates at a certain pressure and temperature if the fugacity of that component in the sample is higher than the fugacity of its pure state at reservoir condition, according to Eq. 1:

$$f_i(P_R, T_R, z_i) - f_i^{\text{pure}}(P_R, T_R) \geq 0. \quad (1)$$

3. Precipitated asphaltene assumed as a pure liquid which is in equilibrium with oil, according to Eq. 2:

$$f_{As}^{\text{pure}}(P, T) = f_{As}^{\text{oil}}(P, T, x_{As}). \quad (2)$$

4. Precipitated asphaltene does not effect on the flash equilibrium of the other phases (remaining oil and gas), according to Eq. 3:

$$f_i^{\text{Oil}}(P, T, x_i) = f_i^{\text{Gas}}(P, T, y_i). \quad (3)$$

By the above assumptions, in the next step, asphaltene precipitation modeling was started with Eq. 4 (general form of the EOS):

$$P = \frac{RT}{V-b} - \frac{a}{V^2}, \quad (4)$$

where “ $a$ ” is the attractive energy and “ $b$ ” is the co-volume parameters for pure species. The evaluations of these parameters have significant importance for the accurate representation of the experimental data and are defined differently in the available EOS. However, general form of “ $a$ ” and “ $b$ ” parameters is presented as Eqs. 5 and 6, respectively:

$$a = \psi \frac{\alpha(T)R^2T_C^2}{P_C} \quad (5)$$

$$b = \Omega \frac{RT_C}{P_C}. \quad (6)$$

It is noticeable that the amount of  $\psi$ ,  $\alpha$ , and  $\Omega$  is defined differently for different EOS. The PR and SRK-EOS as two well-known cubic equations of state are typically used with success mostly for non-polar/slightly polar compounds. As asphaltene is known as the most polar fraction of oil and its precipitation is a function of pressure, temperature, and composition of its surrounding oil sample, PR and SRK-EOS cannot be able to predict its properties correctly.

Asphaltene precipitation starts at high pressures and increases with the reduction of pressure until bubble point pressure, and then, reduces by pressure reduction, below the bubble point pressure (in other words, the bubble point pressure has the maximum amount of asphaltene precipitation). Some authors assumed the amount of asphaltene precipitation as a function of  $(P - P_b)$  (De Boer and Leeriooyer

1992), thus here for calculating  $b$ -parameter,  $\Omega$  assumed as a function of  $(P - P_b)$  and modified-SRK-EOS is derived (Hajizadeh et al. 2020). However, the amount of  $\psi$ ,  $\alpha$ , and  $\Omega$  parameters for PR, SRK, and modified-SRK equations of state are listed in Table 1.

After definition “ $a$ ” and “ $b$ ” parameters for pure species, to apply them for mixtures, some mixing and combining rules are required. Common mixing rule is van der Waals mixing rule that combines the pure parameters ( $a$  and  $b$ ) to achieve mixture parameters as Eqs. 7 and 8:

$$a^{\text{mixture}} = \sum_i \sum_j x_i x_j a_{ij} \quad (7)$$

$$b^{\text{mixture}} = \sum_i x_i b_i. \quad (8)$$

For accounting the cross-term parameter  $a_{ij}$ , some combining rules are needed. Combining rules show the relations between different species in a mixture. Equations 9–11 are different types of combining rules (Ikeda and Schaefer 2011) that give satisfactory results, and to our knowledge, two last have not been used for asphaltene by authors.

- Conventional one-binary interaction parameter:

$$a_{ij} = (a_i a_j)^{0.5} (1 - K_{ij}). \quad (9)$$

- Margules type two-binary interaction parameter:

$$a_{ij} = (a_i a_j)^{0.5} (1 - x_i K_{ij} - x_j K_{ji}). \quad (10)$$

- van Laar type two-binary interaction parameter:

$$a_{ij} = (a_i a_j)^{0.5} \left( 1 - \frac{K_{ij} K_{ji}}{x_i K_{ij} + x_j K_{ji}} \right). \quad (11)$$

Margules and van Laar equations are used in this work, since they can acceptably correlate for complex polar systems with the models, and their parameters are available in commercial simulators for many systems which can also

**Table 1** Parameters of equation of state

	$\Omega$	$\Psi$	$A$
PR <sup>a</sup>	0.07780	0.45724	$[1 + (0.37464 + 1.54226\omega - 0.26992\omega^2)(1 - T_r^{1/2})]^2$
SRK <sup>a</sup>	0.08664	0.42748	$[1 + (0.480 + 1.574\omega - 0.176\omega^2)(1 - T_r^{1/2})]^2$
Modified-SRK <sup>b</sup>	$-1.005 \times 10^{-8}(P - P_b)^2$ $+ 8.455 \times 10^{-7}(P - P_b)$ $+ 8.707 \times 10^{-2}$	0.42748	$[1 + (0.480 + 1.574\omega - 0.176\omega^2)(1 - T_r^{1/2})]^2$

<sup>a</sup>Kontogeorgis and Folas (2010)

<sup>b</sup>Hajizadeh et al. (2020)

be estimated easily from few data (Kontogeorgis and Folas 2010).

Binary interaction parameters of all pairs of species in different equations are listed in Appendix 2.

For modeling asphaltene precipitation, in the first step, the precipitating fractions of the oil sample were determined based on Eq. 1. Each component that satisfies the inequality of Eq. 1 can be assumed as a fraction of precipitation. All components with this property were lumped as a pseudo-component which was fractionated into two new pseudo-components: precipitating component (asphaltene) and non-precipitating component.

Another challenging part in asphaltene precipitation modeling is the determination molecular weight of asphaltene. The asphaltene molecular weight is not unique, but according to literature (Appendix 1), its value has been mostly reported between 500 and 1000 (g/mol), with most probable value around 750 which is taken in this study for asphaltene molecular weight. Then, by knowing the weight percent of asphaltene in dead oil, its mole percent in a live-oil sample was calculated based on Eqs. 12 and 13 and is presented in Table 2:

wt% of Asphaltene in live oil

$$= \text{wt\% of Asphaltene in dead oil} \times \frac{\text{dead oil density}}{\text{dead oil density} + \text{GOR} \times \text{gas density}} \quad (12)$$

mol% of Asphaltene in live oil

$$= \text{wt\% of Asphaltene in live oil} \times \frac{\text{MW of live oil}}{\text{MW of Asphaltene}} \quad (13)$$

Other properties of asphaltene components were set according to Arya et al. (2016). The critical properties of non-precipitating pseudo-component were tuned according to the experimental bubble point pressure of the reservoir oil. For this reason, the critical properties of non-precipitating pseudo-component were assumed and the mole fractions of gas in equilibrium with the reservoir oil at the experimental bubble point pressure were calculated. If the calculated

**Table 2** Properties of precipitating (asphaltene) and non-precipitating pseudo-component

	Asphaltene	Non-precipitating pseudo component
$T_c$ (K)	1040 <sup>a</sup>	900
$P_c$ (bar)	15.44 <sup>a</sup>	16.59
$\Omega$	1.535 <sup>a</sup>	0.665
MW	750	220.1
Mole% in live oil	0.0703	26.04

<sup>a</sup>Arya et al. (2016)

gas mole fractions of all components at bubble point pressure satisfy the equality of Eq. 14, the assumed properties are correct; otherwise, assumptions must be changed until satisfying the equation:

$$\sum y_i^b = 1. \quad (14)$$

All properties of the asphaltene and non-precipitating pseudo-component are presented in Table 2. In addition to the mentioned properties, binary interaction parameters ( $K_{ij}$  and  $K_{ji}$ ) for pairs of asphaltene with other species were needed which tuned with modeling of upper onset pressure (UOP). For this reason, the properties of the pure asphaltene and the asphaltene in the reservoir oil condition were calculated at the experimental UOP of the reservoir oil. If the calculated properties satisfy the equality of Eq. 2, the assumed binary interaction parameters are correct; otherwise, assumptions must be changed until satisfying the equation.

By applying above equations and aforementioned properties, asphaltene precipitation was modeled under different pressures and also for different injection concentrations of

nitrogen and first stage gas which its composition and properties are presented in Tables 3 and 4, respectively.

**Table 3** Composition of first stage gas and reservoir oil

Component	Mole percent (first stage gas)	Mole percent (reservoir oil)
H <sub>2</sub> S	0.92	0.65
N <sub>2</sub>	0.20	0.11
CO <sub>2</sub>	3.06	2.31
C <sub>1</sub>	79.63	53.31
C <sub>2</sub>	7.55	6.60
C <sub>3</sub>	4.57	3.91
i-C <sub>4</sub>	0.74	0.66
n-C <sub>4</sub>	1.57	1.60
i-C <sub>5</sub>	0.49	0.73
n-C <sub>5</sub>	0.58	1.06
C <sub>6</sub>	0.38	2.95
C <sub>7</sub>	0.24	3.30
C <sub>8</sub>	0.05	2.85
C <sub>9+</sub>	0.02	19.96
C <sub>7+</sub>	0.31	26.11



**Table 4** Properties of first stage gas

Molecular weight	22.03
Relative density	0.7606
Net heating value (Btu/SCF)	1124

**Table 5** Properties of reservoir oil

Reservoir temperature	143 °C
Initial reservoir pressure	10,000 psia
Bubble point pressure	4700 psia
Gas/oil ratio (SCF/STB)	1650
Relative density of gas	0.8563
Molecular weight of live oil	69.82
Molecular weight of dead oil	197.46
Relative density of dead oil	0.827
Wt% of asphaltene in dead oil	1.15
Wt% of saturate in dead oil	74.20
Wt% of aromatic in dead oil	20.78
Wt% of resin in dead oil	3.87

## Experimental procedure

There are different methods for measuring the amount of asphaltene precipitation. In this work for investigating the effect of pressure depletion and N<sub>2</sub> injection on the amount of asphaltene precipitation, gravimetric method was used. Gravimetric method is a precise method and the precipitation–pressure plot can be simply defined based on the results of this method (Zendehboudi et al. 2014; Jamaluddin et al. 2002). The main steps of experimental procedure are summarized as follows:

Dead oil sample of the reservoir with composition and properties mentioned Tables 3 and 5, was sent to a PVT cell at reservoir pressure and temperature. Then, the sample was mixed with the desired amount of separated gas from different stages of the production unit according to the GOR of each step; here mixing for each stage continued until gas dissolved in liquid. The final composition of the prepared live oil sample must be in accordance with that is shown in Table 3. After preparing the live oil sample, to make samples with 0, 10, 20, and 40 mol% of N<sub>2</sub> (addition to the initial nitrogen content of reservoir oil), desired amount of N<sub>2</sub> was added to it at reservoir pressure and temperature (to ensure the maximum solution of N<sub>2</sub> in oil, the final sample should be mixed (at least for) about 24 h and even more for higher amounts of N<sub>2</sub> injection).

The pressure of each sample with the desired amount of N<sub>2</sub> content was reduced from 8000 psia (above the upper onset pressure of the reservoir oil) to 3000 psia [below the

lower onset pressure (LOP) of the reservoir oil] with steps of 1000 psi (for each pressure step, the sample was mixed for 30 min and then placed at rest for 72 h until the equilibrium state has been reached).

Finally, a part of sample from the top of the cell was picked and its asphaltene content was measured (if the pressure is below the bubble point pressure, the liberated gas from the oil should be removed and the sample was taken from the top of the liquid in the cell) and the amount of asphaltene precipitation in each sample was calculated based on the difference between the asphaltene content of each samples with asphaltene content of oil reservoir sample. The asphaltene content was measured based on IP/143.

## Results and discussion

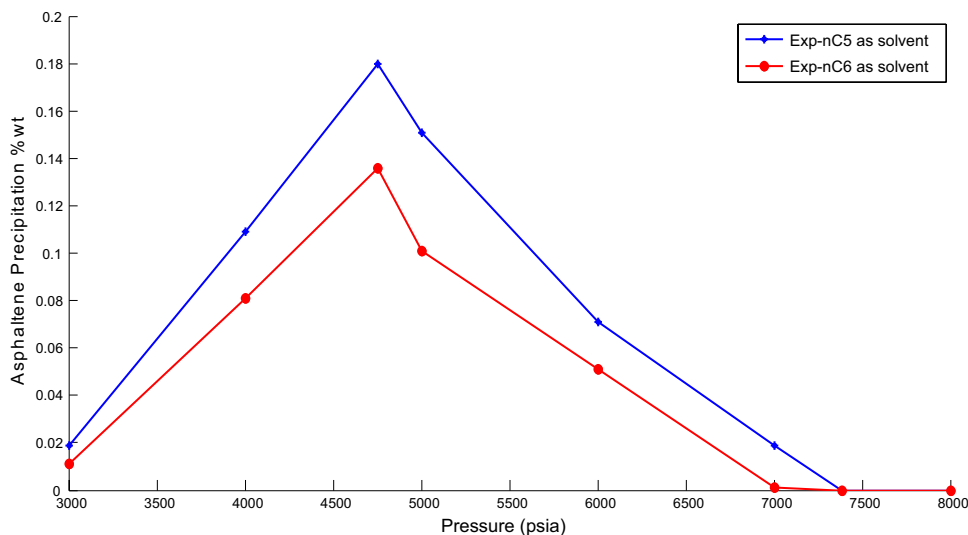
In this study, the amount of asphaltene precipitation during primary production and gas injection (different mole percent of nitrogen and first stage gas) was investigated. The amount of asphaltene precipitation was measured in the laboratory by gravimetric method; and also, predicted by PR, SRK, and modified SRK equations of state.

As illustrates in Fig. 1, the experimental data show that during primary production of the reservoir, asphaltene precipitation starts at high pressure (UOP) and increases with the reduction of pressure until bubble point pressure. Asphaltene precipitation decreases by pressure reduction, below bubble point pressure (i.e., bubble point pressure has maximum asphaltene precipitation) because of evaporation of light gases below bubble point pressure and increasing the capability of the heavier remaining oil to solution asphaltene.

Generally, gas injection into the system reduces the heat of vaporization and increases the molar volume of fluid (oil without asphaltene) which leads to reduction of solubility parameter. Accordance with this fact and as presented in Fig. 2, injection of the first stage gas to the system will increase the amount of asphaltene precipitation. However, as illustrated in Fig. 3 during nitrogen injection to the system, the experimental data show a little complex pattern.

At low pressures, nitrogen injection reduces the amount of asphaltene precipitation in any concentration. This observation shows that at low pressures, oil sample cannot dissolve nitrogen. Nitrogen injection leads to the liberation part of light components from oil and the heavier remaining oil can dissolve more asphaltene. Also, Wang et al. (2018) reported that N<sub>2</sub> injection will not cause serious asphaltene problems. The results of comparison between nitrogen and first stage gas injection are indicated in Fig. 4. This figure shows that at pressures below the 6000 psia, in the same concentration of injected gas, the asphaltene precipitation for first stage gas injection is higher than nitrogen injection.

**Fig. 1** Asphaltene precipitation percent versus pressure (during natural depletion)



This is because of the low molecular weight of first stage gas in comparison with nitrogen.

Since, at high pressures, the ability of oil to dissolve some nitrogen increases, oil becomes lighter and cannot dissolve asphaltene; which results in the increases in precipitation amount. However, it should be noted that at high pressures during low concentration of nitrogen injection, the amount of asphaltene precipitation increases with nitrogen concentration; and for high concentration of injected gas, the scenario is reverse; and the maximum amount of precipitation occurs at about 0.1 mol fraction of injected nitrogen. It shows that the maximum solubility of the nitrogen in the oil sample is about 0.1 mol fractions at high pressures.

During the gas injection process, the bubble point pressure will increase; in other words, it can be concluded that the overall pattern of asphaltene precipitation versus pressure for natural depletion and gas injection process is similar. It was observed from the result that at a pressure equal to 7000 psia and concentration of 0.1 of injected nitrogen, the amount of asphaltene precipitation is higher than when same concentration of first stage gas is injected at the same pressure. It happens, because the pressure of 7000 psia is near the bubble point pressure for the sample with the injection of 0.1 mol fraction of nitrogen (with maximum precipitation) but for the sample with the injection of 0.1 mol fraction of first stage gas is well above the bubble point pressure (near the UOP with minimum precipitation).

In this study for more investigation, the effect of natural pressure depletion and gas injection on the amount of asphaltene precipitation, PR, SRK, and modified-SRK-EOS with different types of combining rules (conventional, Margules, and van Laar type) were used to achieve the best prediction of asphaltene precipitation.

Experimental data of precipitated asphaltene at different situations are listed in Table 6. In addition, Figs. 5, 6, 7 show the standard error bars of the experimental data versus predicted values achieved by both PR and SRK equations of state with conventional, Margules, and van Laar types of combining rules, respectively. In Fig. 5 (i.e., conventional combining rule), both SRK-EOS and PR-EOS have a relatively high deviation from experimental data. However, SRK modeling data have higher accuracy than PR-EOS data. The root-mean-square error (RMSE) of about 76 data point for each EOS is measured by Eq. 15 and the results are listed in Table 7. According to this table, RMSE of modeling by SRK-EOS and PR-EOS with the conventional combining rule are 0.0788 and 0.1116:

$$\text{RMSE} = \sqrt{\frac{\sum_1^n (\text{Exp.data}_i - \text{Cal.data}_i)^2}{n}} \quad (15)$$

As illustrated in Fig. 6, prediction of the amount of asphaltene precipitation when Margules types were used is similar to conventional combining rule both for PR and SRK-EOS. Also, it should be noted that SRK-EOS with Margules type of combining rule shows higher accuracy than PR-EOS; the amount of RMSE of this combining rule for SRK- and PR-EOS is about 0.0734 and 0.0964, respectively. The results show that Margules combining rule in despite of using different binary interaction parameters for a pair of components does not help in improving modeling.

As depicted in Fig. 7, van Laar type combining rule has the least deviation from experimental data rather than other two types of combining rules. As presented in Table 7, the RMSE value of van Laar combining rule is well lower than two other combining rules, and its amount for SRK- and

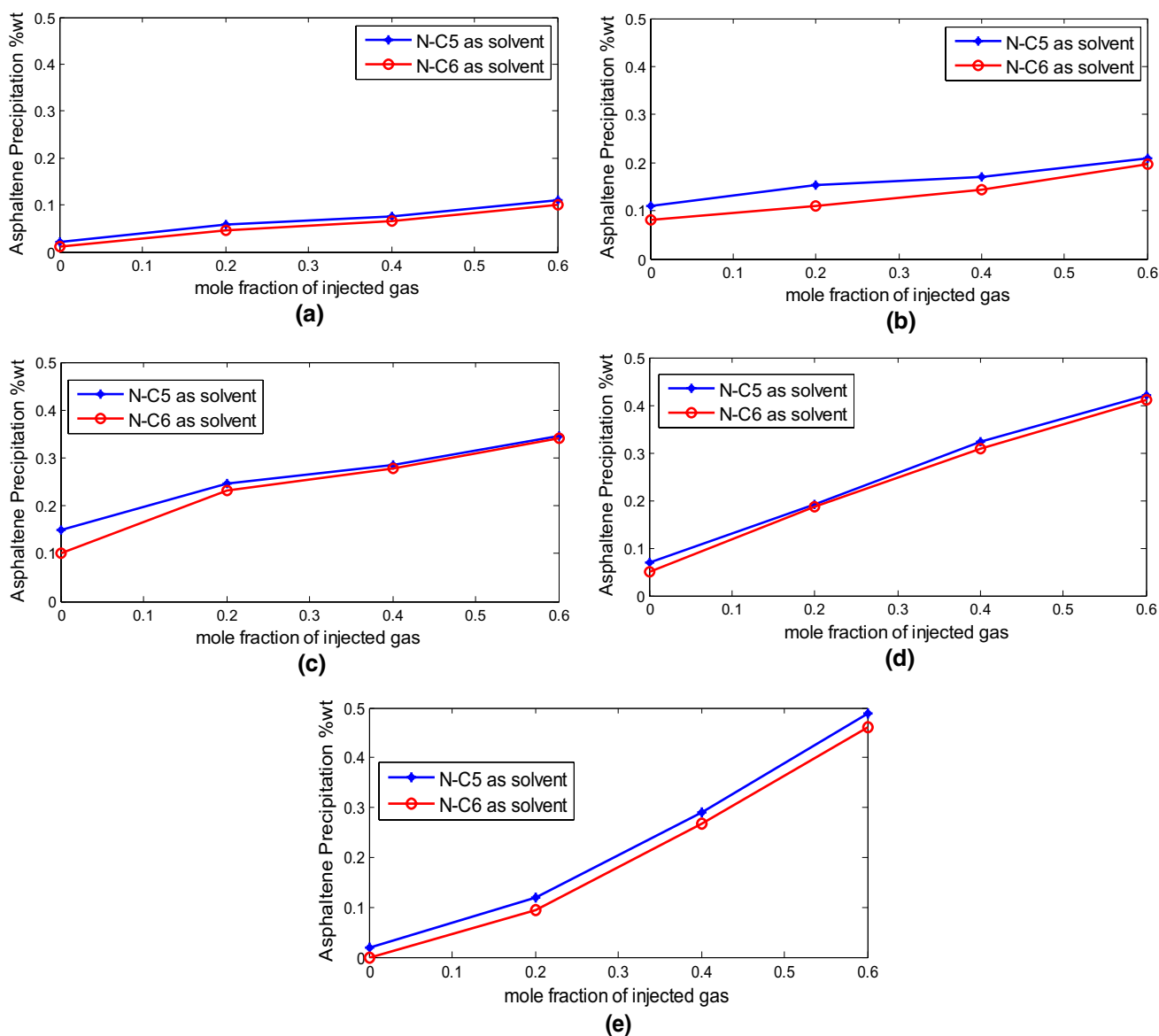


**Fig. 2** Asphaltene precipitation during first stage gas injection at different pressures. **a** 3000; **b** 4000; **c** 5000; **d** 6000; and **e** 7000 psia

PR-EOS is 0.0296 and 0.0623, respectively. The results show that although the van Laar type of combining rule is a complex combining rule, but it could predict the amount of asphaltene precipitation very well.

Based on the literature (De Boer and Leeriooyer 1992),  $(P - P_b)$  is an effective parameter for asphaltene precipitation; thus, in modified SRK-EOS, b-parameter is defined as a function of  $(P - P_b)$ . As presented in Fig. 8, the modified SRK-EOS with conventional and van Laar combining rule can make a better prediction for asphaltene precipitation, with respect to the PR and SRK-EOS.

Figure 8 shows the results of asphaltene precipitation prediction, when modified SRK-EOS with van Laar and conventional types of combining rule is used. As shown in this figure, the Modified-SRK-EOS with van Laar combining rule can predict the experimental data almost correctly but with the conventional combining rule has a bit over estimation from experimental data. The RMSE value of modified-SRK-EOS with different combining rules according to Table 7 is 0.0464, 0.0713, and 0.0292, for conventional, Margules, and van Laar combining rule, respectively. As shown in this table, the SRK-EOS and modified-SRK-EOS



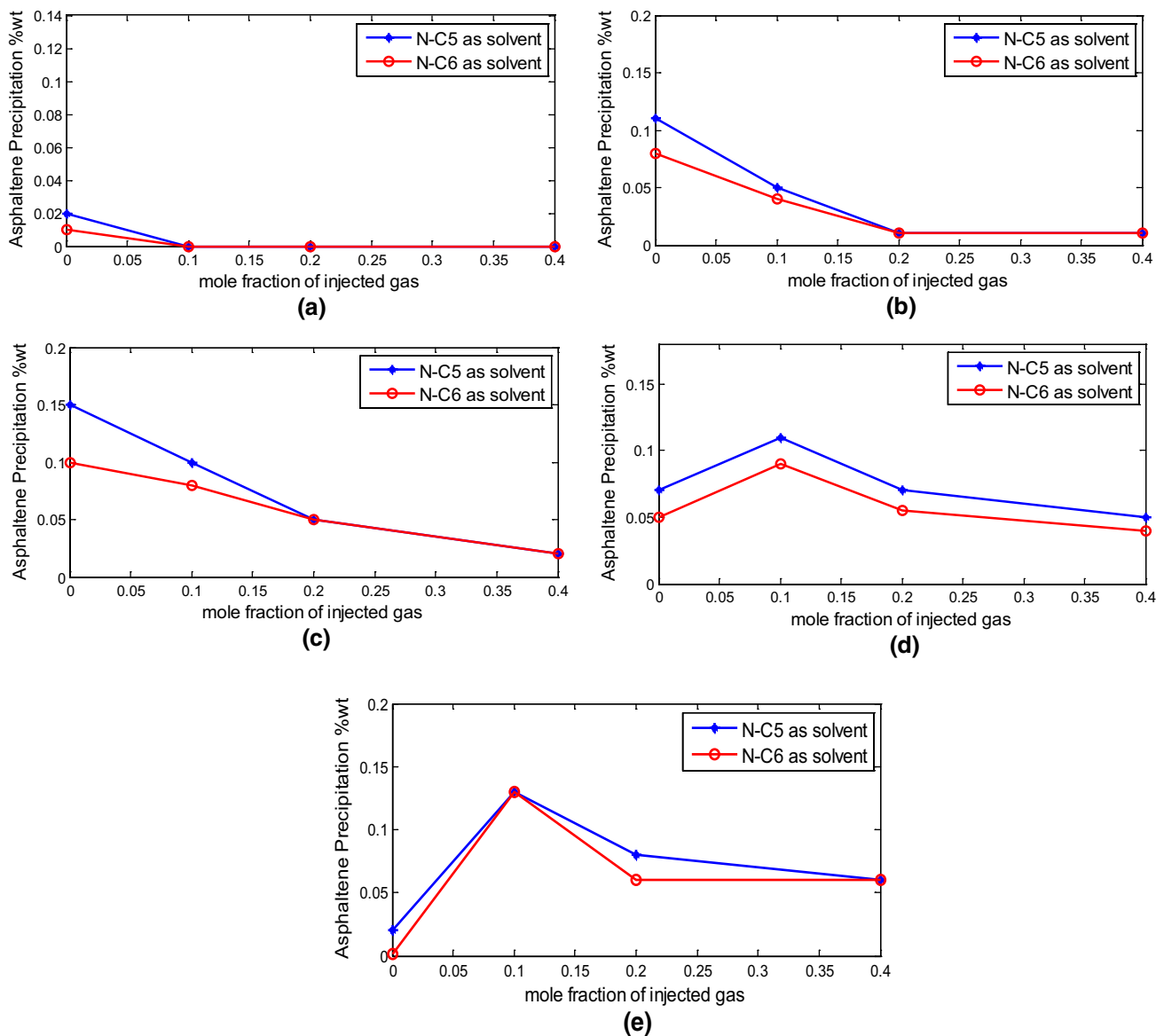


**Fig. 3** Asphaltene precipitation during  $N_2$  injection at different pressures. **a** 3000; **b** 4000; **c** 5000; **d** 6000; and **e** 7000 psia

with van Laar combining rule have the same RMSE value from experimental asphaltene precipitation data.

The modeling of asphaltene precipitation amount with modified-SRK-EOS versus pressure during natural depletion (without injection) is presented in Fig. 9. This figure compares the results of modified-SRK-EOS with conventional and van Laar combining rules. According to this figure, both equations can predict the trend and amount of asphaltene precipitation, correctly. Modified-SRK-EOS with conventional combining rule shows accurate matching with experimental data when n-C<sub>5</sub> has been used as a solvent. While the results of van Laar combining rule lie between the precipitation data from two solvents (n-C<sub>5</sub> and

n-C<sub>6</sub>), it is better matched with the results obtained when n-C<sub>6</sub> was used as a solvent. The same results were recorded by Ikeda and Schaefer 2011, for modeling of water–ethanol system by combination of EOS with different combining rules (containing van Laar, Margules and conventional type). They concluded that using complex combining rules may not always lead to accurate results and it is necessary to consider their combination with EOS and also the characteristics of the system.

Figure 10 shows the results of asphaltene precipitation modeling versus mole fraction of injected nitrogen at different pressures. The modified-SRK-EOS in accordance with experimental data show that at low pressures (3000 and

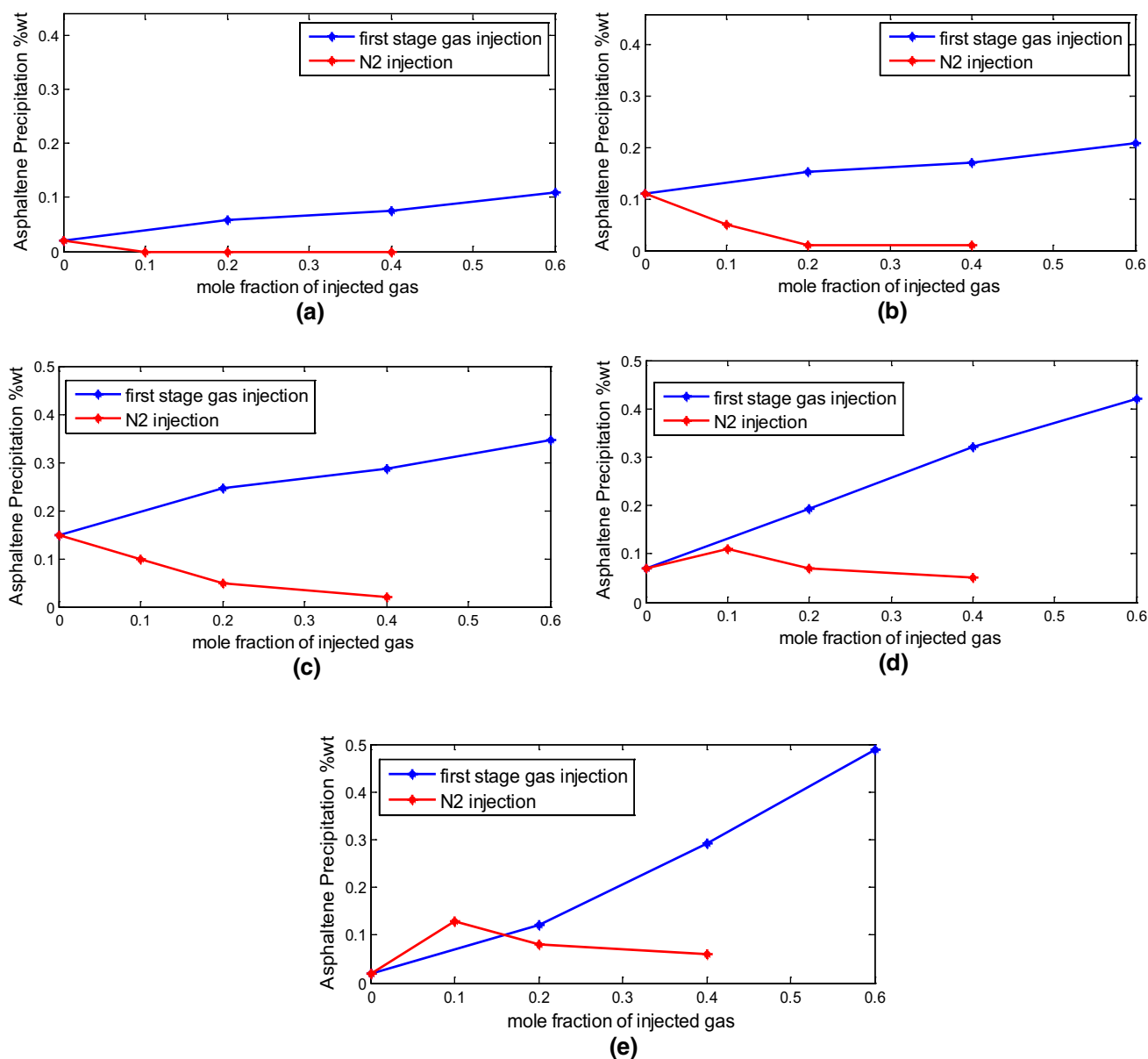


**Fig. 4** Comparison of different gas injection at different pressures. **a** 3000; **b** 4000; **c** 5000; **d** 6000; and **e** 7000 psia

4000 psia), nitrogen injection reduces asphaltene precipitation in any injection concentration. As mentioned before, precipitation reduction happens because of the very low solubility of nitrogen at low pressures. At low pressures, liberation the light gases from oil is the only effect of nitrogen injection which results in more stability of asphaltene in oil, as we know that asphaltene can be more soluble in heavy crude oils.

As presented in Fig. 10 at high pressures (Fig. 10c–e), solubility of nitrogen in crude oil increases. Nitrogen injection increases asphaltene precipitation because of reduction of density and viscosity of crude oil. However, after some concentration of injected nitrogen (maximum solubility of nitrogen in oil), asphaltene precipitation begins to reduction again. Maximum precipitation for higher pressures occurs at a higher concentration of injected gas. However, at high

**Table 6** Experimental precipitation data during different situations

	Natural depletion			First stage gas injection mole fraction			Nitrogen injection mole fraction			Solvent/pressure	
	0	0.2	0.4	0.6	0.1	0.2	0.4				
0.019	0.053	0.08	0.115	0.00	0.00	0.00	n-C <sub>5</sub>	3000			
0.009	0.047	0.07	0.105	0.00	0.000	0.00	n-C <sub>6</sub>				
0.109	0.152	0.176	0.213	0.05	0.01	0.01	n-C <sub>5</sub>	4000			
0.081	0.116	0.146	0.202	0.04	0.01	0.01	n-C <sub>6</sub>				
0.149	0.250	0.286	0.342	0.10	0.05	0.02	n-C <sub>5</sub>	5000			
0.101	0.238	0.284	0.337	0.08	0.05	0.02	n-C <sub>6</sub>				
0.068	0.197	0.327	0.415	0.11	0.07	0.05	n-C <sub>5</sub>	6000			
0.048	0.190	0.313	0.407	0.09	0.055	0.04	n-C <sub>6</sub>				
0.022	0.120	0.296	0.494	0.12	0.11	0.07	n-C <sub>5</sub>	7000			
0.002	0.093	0.272	0.466	0.11	0.10	0.07	n-C <sub>6</sub>				

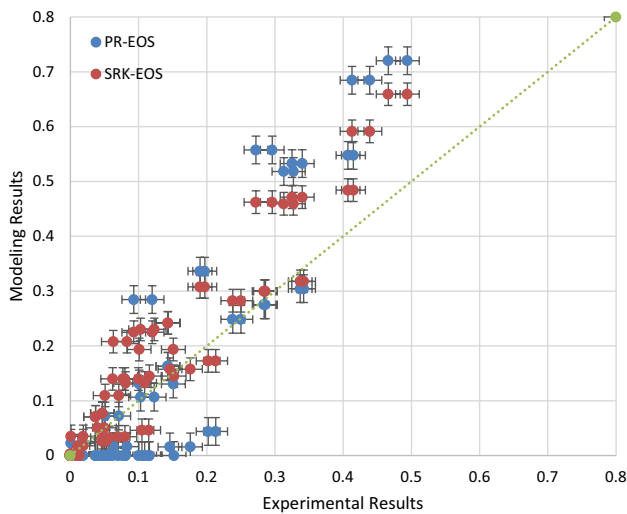


**Fig. 5** Comparison of modeling results with experimental data of asphaltene precipitation (wt%) (conventional combining rule)

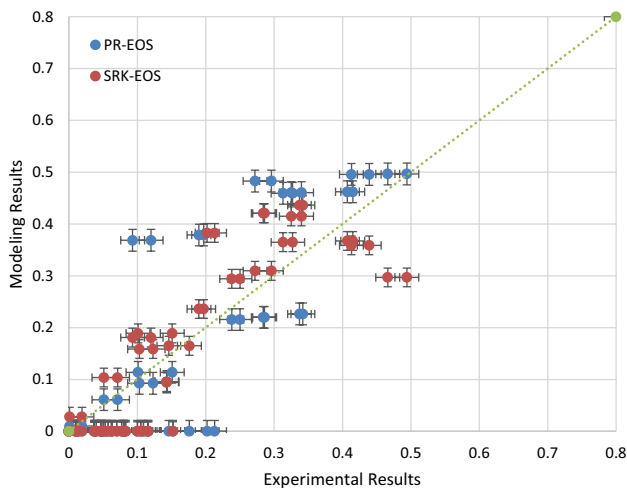


**Fig. 6** Comparison of modeling results with experimental data of asphaltene precipitation (wt%) (Margules combining rule)

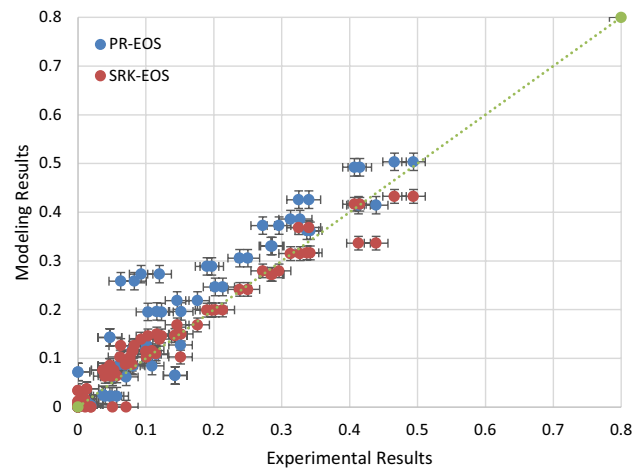


**Fig. 7** Comparison of modeling results with experimental data of asphaltene precipitation (wt%) (van Laar combining rule)

**Table 7** RMSE values for modeling by PR, SRK, and modified-SRK-EOS with different combining rules

	Conventional com. rule	Margules com. rule	van Laar com. rule
PR-EOS	0.1116	0.0964	0.0623
SRK-EOS	0.0788	0.0734	0.0296
Modified-SRK-EOS	0.0464	0.0713	0.0292

pressure (Fig. 10e), precipitation amount is always higher than the amount of precipitation in without injection state.

Figure 11 shows experimental data and modeling with modified-SRK-EOS precipitation during first stage gas injection at different pressures. This figure shows that any concentration of first stage gas injection in comparison to

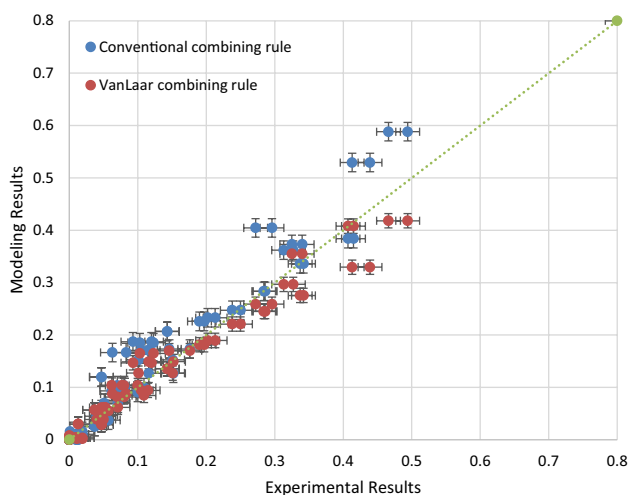


**Fig. 8** Comparison of modeling results with experimental data of asphaltene precipitation (wt%) (modified-SRK-EOS)

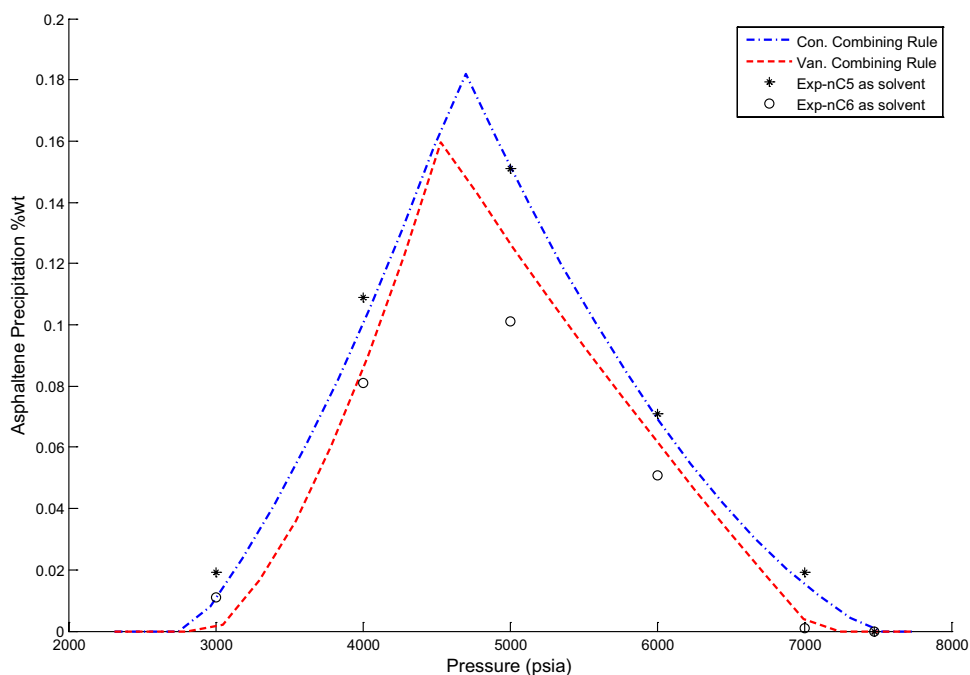
without injection will increase the amount of asphaltene precipitation at any pressure. The modeling results show that higher concentration of injected gas results higher the asphaltene precipitation because of lightening the oil sample. It should be noted that at high pressures and for low concentration of gas injection (left side of Fig. 11c–e), the

precipitation increases rapidly with mole fraction of injected gas, while this increasing for high mole fraction of injected gas at high pressures (right side of Fig. 11c–e) is smooth. As illustrated in this figure for low pressures (Fig. 11a, b), the amount of precipitation increases smoothly with gas concentration. This happens as a result of the liberation of light components from crude oil at high mole fraction of injected gas or at low pressures.

Figures 10 and 11 also compare the two combining rules, conventional and van Laar type. It is deduced from these figures that, for low pressures, both of the equations have the same accuracy. However at high pressures, the high importance of interactions between different components needs more accurate interaction parameter and also a more accurate relation between these parameters to define energy parameter of EOS—“*a*” parameter—therefore at high pressures (Figs. 10c–e, 11c–e), van Laar type—two-binary interaction parameters—combining rule with accurate and distinct interaction parameter of each pair of components can predict the experimental data more accurately. Table 8 shows the performance of each EOS in conjunction with different combining rules for modeling asphaltene precipitation. This table can be a great help for choosing the proper model of asphaltene precipitation in different situations and pressures.

Among all combination of EOS and combining rules, modified-SRK-EOS with van Laar combining rule has high

**Fig. 9** Asphaltene precipitation vs. pressure during primary depletion (modified-SRK-EOS with different combining rules)



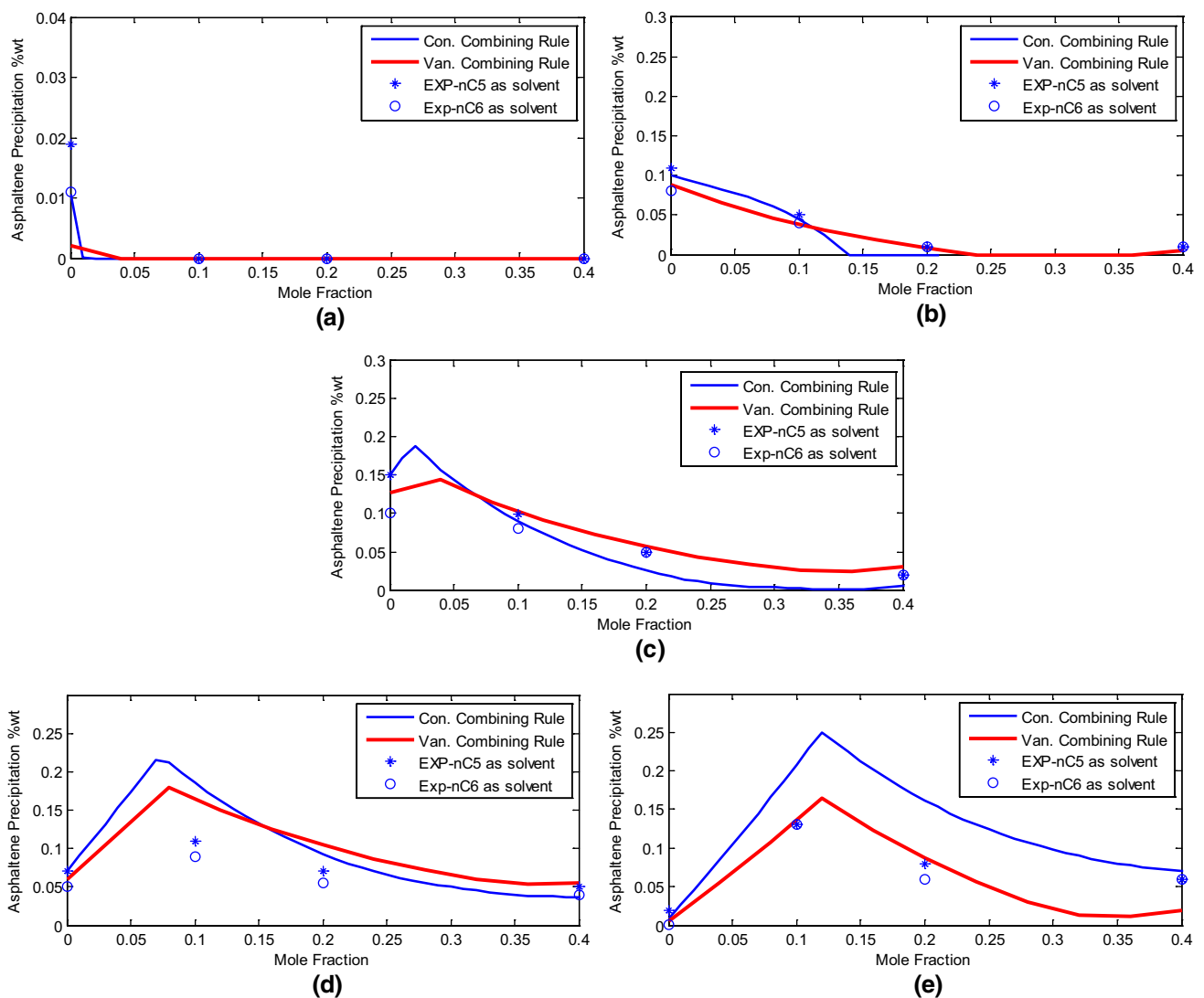


**Fig. 10** Asphaltene precipitation vs. mole fraction of injected gas ( $N_2$ ) at different pressures (modified SRK-EOS with different combining rules). **a** 3000; **b** 4000; **c** 5000; **d** 6000; and **e** 7000 psia

accuracy for all situation (natural depletion, first stage gas, and nitrogen injection) and for all ranges of pressures.

## Conclusions

In this study, the amount of asphaltene precipitation during primary production and gas injection [nitrogen injection (0.1, 0.2 and 0.4 mol fraction) and first stage gas (0.2, 0.4, and 0.6 mol fraction)] in live oil sample was measured

by gravimetric method. Also, three different combining rules, conventional, Margules, and van Laar type, in different EOS (PR, SRK, and modified-SRK) were used and compared. The experimental results show that at low pressures, nitrogen is not soluble in oil and injection of nitrogen reduces asphaltene precipitation because of liberation of light component from crude oil; however, increasing the pressure increases the solubility of nitrogen and increases the asphaltene precipitation. For first stage gas injection, asphaltene precipitation increases at any pressure. Therefore,



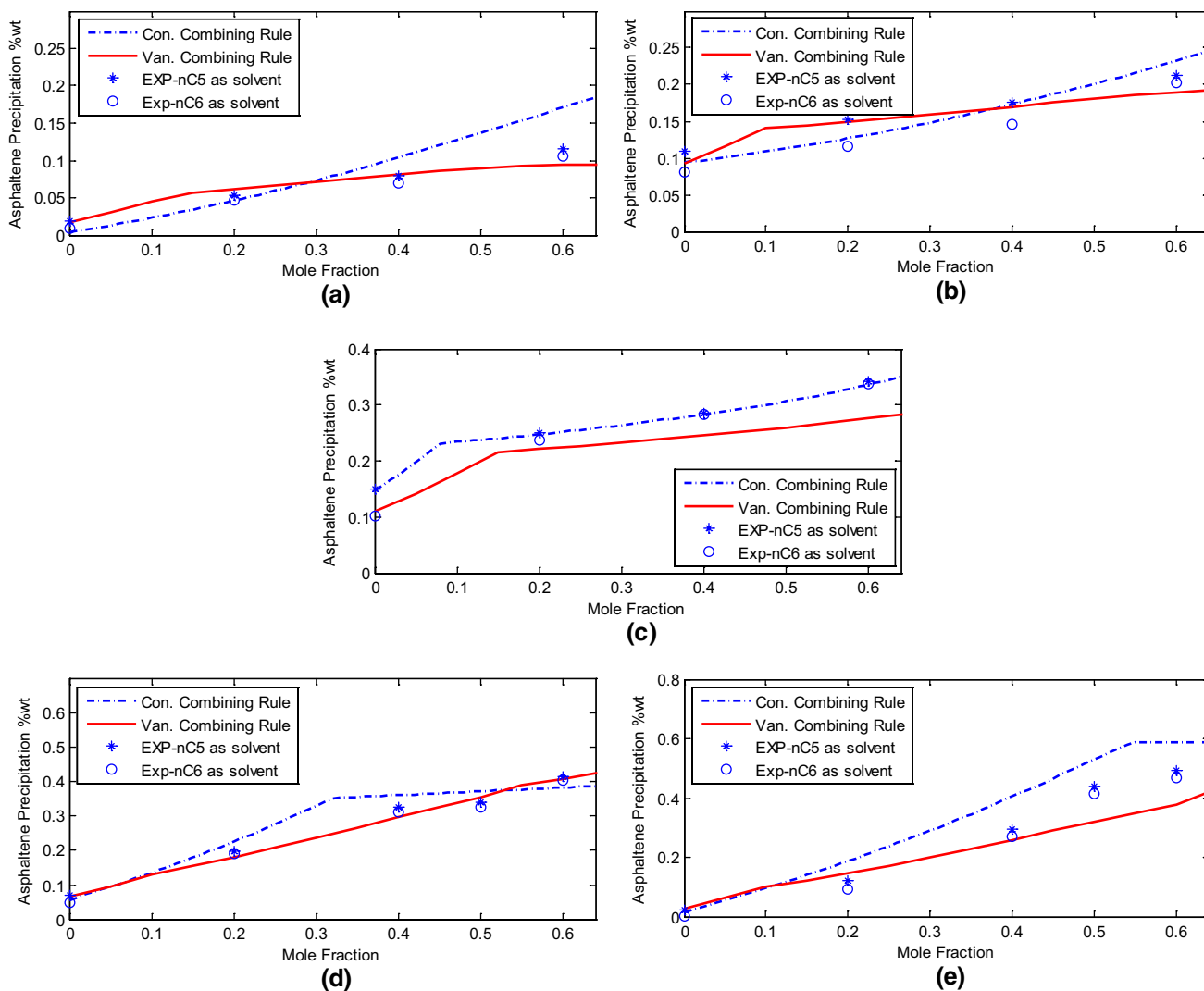


**Fig. 11** Asphaltene precipitation vs. mole fraction of injected gas (first stage gas) at different pressures (modified-SRK-EOS with different combining rules). **a** 3000; **b** 4000; **c** 5000; **d** 6000; and **e** 7000 psia

the amount of asphaltene precipitation due to first stage gas injection is higher than nitrogen injection except at nitrogen concentration and pressures near the bubble point (pressure of 7000 psia and nitrogen injection of 0.1 mol fraction). According to modeling results, van Laar type combining rule can predict the amount of asphaltene precipitation very

well and has the least deviation from experimental data rather than the other two types of combining rules (conventional and Margules combining rule). The  $P - P_b$  parameter can be used to classify different oil samples in terms of the amount of asphaltene precipitation. Modified-SRK-EOS using  $(P - P_b)$  parameter with van Laar combining rule

**Table 8** Proper equations for modeling asphaltene precipitation during different situations

Natural depletion	First stage gas injection		Nitrogen injection		Combining rule	
	PR	Modified	PR	Modified	SRK	Modified
High accuracy for high pressures	High accuracy for low pressures	High accuracy	Moderate accuracy for low pressures	High accuracy for low pressures	High accuracy for low pressures	High accuracy for low pressures
High accuracy for high pressures	Moderate accuracy	Moderate accuracy	Moderate accuracy	Moderate accuracy for low pressures	High accuracy for low pressures	Margules
High accuracy for high pressures	High accuracy for low pressures	High accuracy	Moderate accuracy for low pressures	High accuracy	High accuracy	van Laar

predicts the experimental data correctly at all situations of pressures and different gas injections. However, at low pressures, conventional combining rule in conjugated with modified-SRK-EOS has the same accuracy as van Laar combining rule and because of its simplicity is a better choice at low pressures. At high pressures, the high importance of interactions between different components needs more accurate interaction parameter and also a more accurate relation between these parameters to define energy parameter of EOS—“*a*” parameter—therefore at these pressures, conventional combining rule can not model the results correctly and van Laar equation will be selected.

## Appendix 1: Asphaltene molecular weight

Asphaltene is a self-association molecule that makes very hard to measuring the accurate molecular weight of it. However, there are many works done for measuring the molecular weight of asphaltene. The results of several important works done on this issue with different experimental methods are shown in Table 9 and Fig. 12.

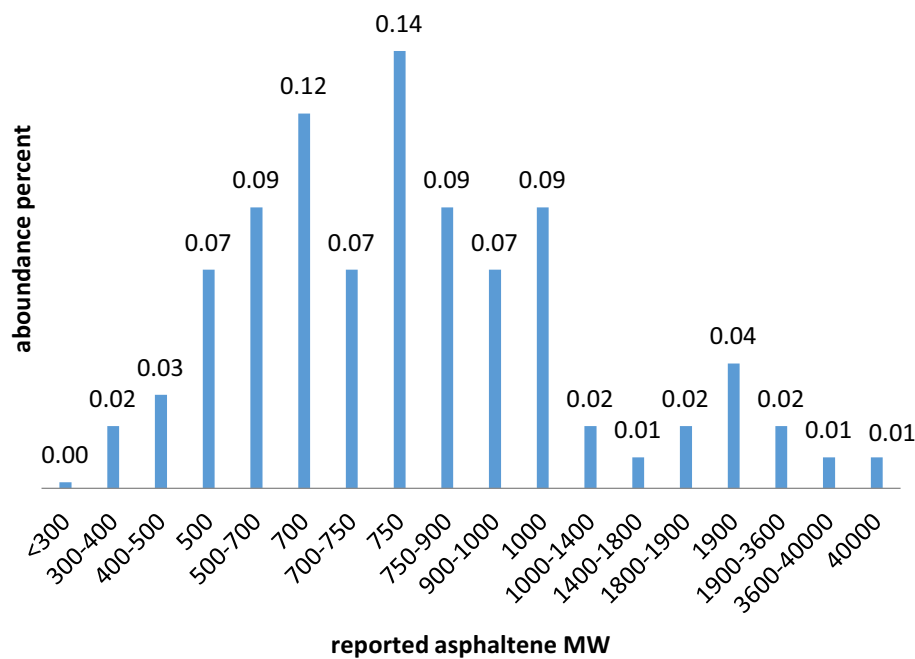
## Appendix 2: Binary interaction parameters

Equations of state need some binary interaction coefficients to be applicable for mixtures. In this section, binary interaction parameters for different combining rules and different EOS are presented.

1. One-binary interaction parameter (conventional combining rule).  
In this type of combining rule, one-binary interaction parameter is used for each pair of components (i.e.,  $K_{ij} = K_{ji}$ ).  
Binary interaction coefficients for common pairs of material containing light hydrocarbons for conventional combining rule are available in the literatures (Arya et al. 2017; Hustad et al. 2014). Binary interaction coefficients for asphaltene with other hydrocarbons are calculated according to experimental data available for upper onset pressure of reservoir oil (Hajizadeh et al. 2020) and are presented in Table 10.
2. Two-binary interaction parameters (Margules type and van Laar type combining rules).  
In this type of combining rules, two-binary interaction parameters are used for each pair of components (i.e.,  $K_{ij} \neq K_{ji}$ ). For this type of combining rule, there is a semi-empirical correlation for binary interaction parameter as Eq. 16 (Fateen et al. 2013):

**Table 9** Reviews and experimental works for determination of asphaltene molecular weight

MW of asphaltene	References	Method
500	Miller et al. (1998)	LD-MS
400–900	Cunico et al. (2004)	APCI-MS
600–700	Pomerantz et al. (2015)	LDI-MS and SALDI-MS
500–1000	Zeinali Hasanvand et al. (2018) and Rastgoo and Kharrat (2017)	TR-FD
400–1200	Merdrignac et al. (2004)	SEC-MS
750–1000	Mullins et al. (2008)	
800–1000	Hutado et al. (2007)	LDI-MS
1000	Aske et al. (2002) and Qian et al. (2007)	FD-FI-MS
1900	Jafari Behbahani et al. (2011)	GPC
700–40,000	Soleymanzadeh et al. (2018)	
3200 ± 400	Acevedo et al. (2005)	
300–1400	Akbarzadeh et al. (2007) and Rodgers and Marshall (2007)	FT-ICR-MS
750	Subramanian et al. (2016), Mullins et al. (2012), Badre et al. (2006) and Andrews et al. (2006)	FD-MS FCS
Less than 1000	Arya et al. (2016)	
1000–30,000	Barrera et al. (2013)	

**Fig. 12** Abundance of asphaltene molecular weight according to Table 9

**Table 10** Binary interaction parameter ( $K_{ij}$ )

	CO <sub>2</sub> <sup>a</sup>	H <sub>2</sub> S <sup>a</sup>	N <sub>2</sub> <sup>a</sup>	Asphaltene
CO <sub>2</sub>				0.22 <sup>b</sup>
H <sub>2</sub> S	0.0989			0 <sup>b</sup>
N <sub>2</sub>	-0.0315	0.1696		0.33 <sup>b</sup>
C <sub>1</sub>	0.12	0.08	0.0278	0.252 <sup>c</sup> - 0.145 <sup>d</sup> - 0.148 <sup>e</sup>
C <sub>2</sub>	0.12	0.0852	0.0407	0.252 <sup>c</sup> - 0.145 <sup>d</sup> - 0.148 <sup>e</sup>
C <sub>3</sub>	0.12	0.0885	0.0763	0.252 <sup>c</sup> - 0.145 <sup>d</sup> - 0.148 <sup>e</sup>
i-C <sub>4</sub>	0.12	0.0511	0.0944	0.252 <sup>c</sup> - 0.145 <sup>d</sup> - 0.148 <sup>e</sup>
n-C <sub>4</sub>	0.12	0.06	0.07	0.252 <sup>c</sup> - 0.145 <sup>d</sup> - 0.148 <sup>e</sup>
i-C <sub>5</sub>	0.12	0.06	0.0867	0.252 <sup>c</sup> - 0.145 <sup>d</sup> - 0.148 <sup>e</sup>
n-C <sub>5</sub>	0.12	0.068	0.0878	0.252 <sup>c</sup> - 0.145 <sup>d</sup> - 0.148 <sup>e</sup>
C <sub>6</sub>	0.12	0.05	0.08	0.252 <sup>c</sup> - 0.145 <sup>d</sup> - 0.148 <sup>e</sup>
C <sub>7+</sub>	0.1	0.05	0.13	0.252 <sup>c</sup> - 0.145 <sup>d</sup> - 0.148 <sup>e</sup>

<sup>a</sup>Hustad et al. (2014)<sup>b</sup>Arya et al. (2017)<sup>c</sup>Interaction parameter fitted for PR-EOS<sup>d</sup>Interaction parameter fitted for SRK-EOS<sup>e</sup>Interaction parameter fitted for modified-SRK-EOS

$$K_{ij} = 1 - \frac{1}{2} \frac{b_j}{b_i} \sqrt{\frac{a_i}{a_j}} - \frac{1}{2} \frac{b_i}{b_j} \sqrt{\frac{a_j}{a_i}} + \frac{1}{2} \frac{b_j RT}{\sqrt{a_i a_j}} \frac{\theta_1}{T_{r_i}^{\theta_2} P_{r_i}^{\theta_3}} \quad (16)$$

This equation is applicable for PR-EOS with adjustable parameters  $\theta_1$ ,  $\theta_2$ , and  $\theta_3$  which, for some pair of species, are presented by Fateen et al. (2013) and for other species are adjusted in this study. These parameters are listed in Table 11.

For calculation of binary interaction parameters for SRK-EOS and modified-SRK-EOS, we used the relation between the binary interaction parameter of PR- and SRK-EOS according to Eq. 17 (Jaubert and Privat 2010):

$$K_{ij}^{\text{SRK}} = \frac{2\xi K_{ij}^{\text{PR}} \delta_i^{\text{PR}} \delta_j^{\text{PR}} + \xi (\delta_i^{\text{PR}} - \delta_j^{\text{PR}})^2 - (\delta_i^{\text{SRK}} - \delta_j^{\text{SRK}})^2}{2\delta_i^{\text{SRK}} \delta_j^{\text{SRK}}} \quad (17)$$

$$\delta_i = \frac{\sqrt{a_i}}{b_i} \quad (18)$$

$$\xi \propto \left(\frac{1}{\Omega}\right). \quad (19)$$

The difference between binary interaction of SRK and modified-SRK-EOS is the amount of “ $\delta_{\text{Asp}}$ ” parameter because of difference in “ $b$ ” parameter of these two EOS, according to Table 1.

Also the amount of “ $\xi$ ” in Jaubert and Privat (2010), assumed to be constant about 0.807341 for SRK-EOS, we changed it to  $\xi = 0.794$  for modified-SRK-EOS according to Eq. (19).

**Table 11**  $\theta_1$ ,  $\theta_2$ , and  $\theta_3$  for calculation of binary interaction parameter ( $K_{ij}$ ) of PR-EOS (the parameters in the left side of diagonal line are for Margules and in the right side are for van Laar)

Comp. 1	Comp. 2													
		Asp*	Non-pre	C <sub>6</sub>	n-C <sub>5</sub>	i-C <sub>5</sub>	n-C <sub>4</sub>	i-C <sub>4</sub>	C <sub>3</sub>	C <sub>2</sub>	C <sub>1</sub>	N <sub>2</sub>	H <sub>2</sub> S	
CO <sub>2</sub>	$\theta_1$	2.79*	1.43*	1.319	1.308	1.004	1.397	1.155	1.408	1.424	2.552	2.986	0.97*	
	$\theta_2$	2.27*	2.21*	1.124	0.730	-0.61	1.190	-0.53	0.255	-1.97	0.807	0.725	0.061*	
	$\theta_3$	0.00*	-0.01*	0.079	0.079	0.180	0.047	0.041	0.074	0.5114	0.082	0.112	0.00*	
H <sub>2</sub> S	$\theta_1$	0.38*	4.47*	1.113	1.175	1.804*	0.801	0.922	0.0002*	2.461	2.187	10.60		4.72*
	$\theta_2$	2.71*	1.29*	1.478	0.594	5.625*	-2.53	-3.53	-80.30*	0.807	0.000	1.414		16.4*
	$\theta_3$	0.00*	0.17*	0.025	0.036	0.000*	0.446	0.496	0.000*	-0.063	-0.00	-0.05		0.00*
N <sub>2</sub>	$\theta_1$	7.47*	2.35*	6.849	2.043	1.573*	4.515	1.498*	2.026	1.818	0.866		10.60	2.986
	$\theta_2$	1.37*	1.36*	2.040	0.988	1.002*	1.989	0.938*	0.958	1.179	0.436		1.414	0.725
	$\theta_3$	0.00*	0.002*	0.104	0.156	0.000*	0.033	0.000*	0.112	0.120	-0.01		-0.05	0.112
C <sub>1</sub>	$\theta_1$	25.0*	0.002*	0.471	0.389	0.014*	0.262	0.160	0.211	0.256		0.866	2.187	2.552
	$\theta_2$	1.64*	2.65*	1.272	1.482	0.001*	2.706	-0.88	-0.08	1.086		0.436	0.000	0.807
	$\theta_3$	0.00*	0.14*	0.126	0.104	0.000*	0.008	0.222	0.167	-0.221		-0.01	-0.00	0.082
C <sub>2</sub>	$\theta_1$	21.6*	0.18*	0.062	0.319	0.020*	0.316	0.072	0.002		0.256	1.818	2.461	1.424
	$\theta_2$	1.94*	2.01*	2.031	-0.11	1.894*	0.218	-5.00	-0.90		1.086	1.179	0.807	-1.97
	$\theta_3$	0.00*	0.15*	0.000	-2.51	0.000*	-1.96	0.863	-4.05		-0.22	0.120	-0.063	0.511
C <sub>3</sub>	$\theta_1$	20.6*	0.076*	0.041*	0.007*	0.452	0.001*	-0.21		0.002	0.211	2.026	0.88*	1.408
	$\theta_2$	1.98*	2.07*	2.177*	1.962*	3.899	1.795*	3.857		-0.90	-0.08	0.958	-0.01*	0.255
	$\theta_3$	0.00*	0.00*	0.000*	0.000*	-0.90	0.000*	-0.92		-4.05	0.167	0.112	0.00*	0.074
i-C <sub>4</sub>	$\theta_1$	20.8*	0.029*	0.009*	0.0006*	0.0001*	0.007*		-0.21	0.072	0.160	1.72*	0.922	1.155
	$\theta_2$	1.92*	2.01*	2.056*	1.556*	1.623*	0.006*		3.857	-5.00	-0.88	0.29*	-3.53	-0.53
	$\theta_3$	0.00*	0.00*	0.000*	0.000*	0.000*	0.000*		-0.92	0.863	0.222	0.00*	0.496	0.041
n-C <sub>4</sub>	$\theta_1$	19.8*	0.059*	0.029*	0.003*	0.005*		0.250*	-0.0005*	0.316	0.262	4.515	0.801	1.397
	$\theta_2$	2.01*	2.12*	2.39*	2.197*	2.458*		1.821*	0.560*	0.218	2.706	1.989	-2.53	1.190
	$\theta_3$	0.00*	0.00*	0.00*	0.000*	0.000*		0.000	0.000*	-1.96	0.008	0.033	0.446	0.047
i-C <sub>5</sub>	$\theta_1$	20.1*	0.03*	0.01*	0.0003*		0.0021*	0.0009*	0.452	-0.004*	0.088*	1.90*	0.76*	1.004
	$\theta_2$	1.96*	2.08*	2.35*	1.15*		0.410*	0.640*	3.899	0.103*	0.49*	1.00*	0.18*	-0.61
	$\theta_3$	0.00*	0.00*	0.00*	0.00*		0.000*	0.000*	-0.90	0.002*	0.00*	0.00*	0.00*	0.180
n-C <sub>5</sub>	$\theta_1$	19.8*	0.035*	0.013*		0.0004*	0.0005*	0.0026*	-0.0014*	0.319	0.389	2.043	1.175	1.308
	$\theta_2$	1.98*	2.11*	2.51*		0.870*	0.460*	0.500*	0.510*	-0.11	1.482	0.988	0.594	0.730
	$\theta_3$	0.00*	0.00*	0.00*		0.000*	0.000*	0.000*	0.000*	-2.51	0.104	0.156	0.036	0.079
C <sub>6</sub>	$\theta_1$	21.3*	0.006*		0.0013*	-0.0001*	0.0039*	-0.001*	-0.0012*	0.062	0.471	6.849	1.113	1.319
	$\theta_2$	1.86*	1.98*		0.420*	0.470*	0.440*	0.540*	0.480*	2.031	1.272	2.040	1.478	1.124
	$\theta_3$	0.00*	0.00*		0.000*	0.000*	0.000*	0.000*	0.000*	0.000	0.126	0.104	0.025	0.079
Non-pre	$\theta_1$	1.982		-0.019*	-0.008*	-0.010*	-0.006*	-0.014*	-0.0123*	-0.02*	0.052*	4.62*	0.73*	3.05*
	$\theta_2$	1.490		0.490*	0.480*	0.490*	0.470*	0.520*	0.490*	0.411*	0.51*	0.74*	0.34*	0.42*
	$\theta_3$	0.000		0.000*	0.000*	0.000*	0.000*	0.000*	0.000*	0.004*	0.00*	0.00*	0.00*	0.00*
Asp	$\theta_1$		4.15*	9.343*	2.838*	2.806*	2.381*	2.458*	1.9797*	1.559*	1.50*	15.8*	0.038*	13.1*
	$\theta_2$		0.58*	0.510*	0.500*	0.500*	0.490*	0.090*	0.500*	0.510*	0.54*	0.72*	0.37*	0.44*
	$\theta_3$		0.00*	0.000*	0.000*	0.000*	0.000*	0.000*	0.000*	0.000*	0.00*	0.00*	0.00*	0.00*
		Asp	Non-pre	C <sub>6</sub>	n-C <sub>5</sub>	i-C <sub>5</sub>	n-C <sub>4</sub>	i-C <sub>4</sub>	C <sub>3</sub>	C <sub>2</sub>	C <sub>1</sub>	N <sub>2</sub>	H <sub>2</sub> S	CO <sub>2</sub>

Interaction parameters with \* are fitted in this work; others are adopted from Fateen et al. (2013)



## References

- Abedini R, Abedini A (2011) Development of an artificial neural network algorithm for the prediction of asphaltene precipitation. *Pet Sci Technol* 29:1565–1577
- Abedini A, Ashoori S, Torabi F (2011) Reversibility of asphaltene precipitation in porous and non-porous media. *Fluid Phase Equilib* 308:129–134
- Acevedo S, Gutierrez L, Negrin G, Pereira J, Mendez B, Delolme F, Dessalces G, Broseta D (2005) Molecular weight of petroleum asphaltenes: a comparison between mass spectrometry and vapor pressure osmometry. *Energy Fuels* 19(4):1548–1560
- Ahmadi MA (2012) Neural network based unified particle swarm optimization for prediction of asphaltene precipitation. *Fluid Phase Equilib* 314:46–51
- Akbarzadeh K, Hammami A, Kharrat A, Zhang D, Allenson S, Creek J, Kabir S, Jamaluddin A, Marshall A, Rodgers R (2007) Asphaltenes-problematic but rich in potential. *Oilfield Rev* 19(2):22–43
- Andrews AB, Guerra R, Sen PN, Mullins OC (2006) Diffusivity of asphaltene molecules by fluorescence correlations spectroscopy. *J Phys Chem* 110:8095
- Arya A, Liang X, Von Solms N, Kontogeorgis GM (2016) Modeling of asphaltene onset precipitation conditions with cubic plus association (CPA) and perturbed chain statistical associating fluid theory (PC-SAFT) equations of state. *Energy Fuels* 30(8):6835–6852
- Arya A, Liang X, von Solms N, Kontogeorgis GM (2017) Prediction of gas injection effect on asphaltene precipitation onset using the cubic and cubic-plusassociation equations of state. *Energy Fuels* 31(3):3313–3328
- Ashoori S, Balavi A (2014) An investigation of asphaltene precipitation during natural production and the CO<sub>2</sub> injection process. *Pet Sci Technol* 32(11):1283–1290
- Ashoori S, Abedini A, Abedini R, Qorbani Nasheghi Kh (2010) Comparison of scaling equation with neural network model for prediction of asphaltene precipitation. *J Pet Sci Eng* 72:186–194
- Aske N, Kallevik H, Johnsen EE, Sjoblom J (2002) Asphaltene aggregation from crude oils and model systems studied by high-pressure NIR spectroscopy. *Energy Fuels* 16:1287–1295
- Badre S, Carla C, Norinaga K, Gustavson G, Mullins OC (2006) Molecular size and weight of asphaltene and asphaltene solubility fractions from coals, crude oils and bitumen. *Fuel* 85:1–11
- Barrera DM, Ortiz DP, Yarranton HW (2013) Molecular weight and density distribution of asphaltene from crude oils. *Energy Fuels* 27:2472–2487
- Bouhadda Y, Bormann D, Sheu E, Bendedouch D, Krallafa A, Daou M (2007) Characterization of Algerian Hassi-Messaoud asphaltene structure using Raman-spectrometry and X-ray diffraction. *Fuel* 86:1855–1864
- Buenrostro-Gonzalez E, Lira-Galeana C, Gil-Villegas A, Wu J (2004) Asphaltene precipitation in crude oils: theory and experiments. *AIChE J* 50:2552–2570
- Cunico RI, Sheu EY, Mullins OC (2004) Molecular weight measurement of UG8 asphaltene using APCI mass spectrometry. *Pet Sci Technol* 22:787–798
- De Boer RB, Leerlooyer K, Eigner MR, Van Bergen AR (1992) SPE 24987 screening of crude oils for asphalt precipitation: theory, practice, and the selection of inhibitors. In: European petroleum conference, pp. 259
- Duda Y, Lira-Galeana C (2006) Thermodynamics of asphaltene structure and aggregation. *Fluid Phase Equilib* 241:257–267
- Fateen SEK, Khalil MM, Elnabawy AO (2013) Semi-empirical correlation for binary interaction parameters of the Peng–Robinson equation of state with the van der Waals mixing rules for the prediction of high-pressure vapor–liquid equilibrium. *J Adv Res* 4:137–145
- Hajizadeh N, Moradi GR, Ashoori S (2020) Modified SRK equation of state for modeling asphaltene precipitation. *J Chem React Eng* 18(3)
- Hemmati-Sarapardeh A, AliPour-Yeganeh-Marand R, Naseri A, Safiabad A, Gharagheizi F, Ilani-Kashkouli P, Mohammadi AH (2013) Asphaltene precipitation due to natural depletion of reservoir: determination using a SARA fraction based intelligent model. *Fluid Phase Equilib* 354:177–184
- Hustad OS, Jia N, Pedersen KS, Memon A, Leekumjorn S (2014) High-pressure data and modeling results for phase behavior and asphaltene onsets of Gulf of Mexico oil mixed with nitrogen. *SPE Reservoir Eval Eng* 17(03):384–395
- Hutado P, Hortal AR, Martinez-Haya B (2007) MALDI detection of carbonaceous compounds in ionic liquid matrices. *Mass Spectrom* 21:3161–3164
- Ikeda MK, Schaefer LA (2011) Examination the effect of binary interaction parameters on VLE modeling using cubic equations of state. *Fluid Phase Equilib* 305:233–237
- Jafari Behbahani T, Ghotbi C, Taghikhani V, Shahrabadi A (2011) Experimental investigation and thermodynamic modeling of asphaltene precipitation. *Sci Iran* 18(6):1384–1390
- Jamaluddin AKM, Creek J, Kabir CS, Mcfadden JD, D’Cruz D, Manakalathil J, Joshi N, Ross B (2002) Laboratory techniques to measure thermodynamic asphaltene instability. *J Can Pet Technol* 41(07)
- Jaubert JN, Privat R (2010) Relationship between the binary interaction parameters ( $k_{ij}$ ) of the Peng–Robinson and those of the Soave–Redlich–Kwong equations of state: application to the definition of the PR2SRK model. *Fluid Phase Equilib* 295:26–37
- Kontogeorgis GM, Folas GK (2010) Thermodynamic models for industrial applications. Wiley, New York
- Merdrignac I, Desmazieres B, Terrier P, Delobel A, Laprevote O (2004) Analysis of raw and hydrotreated asphaltenes using off-line and on-line SEC/MS coupling. In: Proceedings of the Heavy Organic Deposition, Los Cabos, Baja California, Mexico
- Miller JT, Fisher RB, Thiyagarajan P, Winans RE, Hunt JE (1998) Sub-fractionation and characterization of Mayan asphaltene. *Energy Fuels* 12:1290–1298
- Mohammadi AH, Richon D (2007) A monodisperse thermodynamic model for estimating asphaltene precipitation. *AIChE J* 53:2940–2947
- Mullins OC, Martínez-Haya B, Marshall AG (2008) Contrasting perspective on asphaltene molecular weight. This comment vs the overview of A.A. Herod, K.D. *Energy Fuels* 22(3):1765–1773
- Mullins OC, Sabbah H, Eyssautier J, Pomerantz AE, Barré L, Andrews AB, Ruiz-Morales Y, Mostowfi F, McFarlane R, Goual L, Lepkovicz R (2012) Advances in asphaltene science and the Yen–Mullins model. *Energy Fuels* 26(7):3986–4003
- Orangi HS, Modarress H, Fazlali A, Namazi MH (2006) Phase behavior of binary mixture of asphaltene + solvent and ternary mixture of asphaltene + solvent + precipitant. *Fluid Phase Equilib* 245:117–124
- Pazuki GR, Nikookar M, Omidkhan MR (2007) Application of a new cubic equation of state to computation of phase behavior of fluids and asphaltene precipitation in crude oil. *Fluid Phase Equilib* 254:42–48
- Peramanu S, Singh C, Agrawala M, Yarranton HW (2001) Investigation on the reversibility of asphaltene precipitation. *Energy Fuels* 15:910–917
- Pomerantz AE, Wu Q, Mullins OC, Zare RN (2015) Laser-based mass spectrometric of asphaltene molecular weight, molecular architecture and nanoaggregate number. *Energy Fuels* 29:2833–2842
- Qian K, Edwards KE, Siskin M, Olmstead WN, Mennito AS, Dechart GJ, Hoosain NE (2007) Desorption and ionization of heavy petroleum molecules and measurement of molecular weight distribution. *Energy Fuels* 21:1042–1047

- Rastgoo A, Kharrat R (2017) Investigation of asphaltene deposition and precipitation in production tubing. *Int J Clean Coal Energy* 6:14–29
- Rodgers RP, Marshall AG (2007) Petroleomics: advanced characterization of petroleum-derived materials by Fourier transform ion cyclotron resonance mass spectrometry (FT-ICR MS). In: *Asphaltenes, heavy oils, and petroleomics*: Springer; p. 63–93
- Sabbagh O, Akbarzadeh K, Badamchi-Zadeh A, Svrcek WY, Yarranton HW (2006) Applying the PR-EOS to asphaltene precipitation from *n*-alkane diluted heavy oils and bitumens. *Energy Fuels* 20:625–634
- Shirani B, Nikazar M, Naseri A, Mousavi-Dehghani SA (2012) Modeling of asphaltene precipitation utilizing association equation of state. *Fuel* 93:59–66
- Soleymanzadeh A, Yousefi M, Kord S, Mohammadzadeh O (2019) A review on methods of determining onset of asphaltene precipitation. *J Pet Explor Prod Technol* 9(2):1375–1396
- Subramanian S, Simon S, Sjoblom J (2016) Asphaltene precipitation models: a review. *Dispers Sci Technol* 37:1027–1049
- Thomas F, Bennion D, Bennion D, Hunter B (1992) Experimental and theoretical studies of solids precipitation from reservoir fluid. *J Can Pet Technol* 31(01)
- Wang P, Zhao F, Hou J, Lu G, Zhang M, Wang Zh (2018) Comparative analysis of CO<sub>2</sub>, N<sub>2</sub> and gas mixture injection on asphaltene deposition pressure in reservoir conditions. *Energies* 11(9):2483
- Zeinali Hasanvand M, Montazeri M, Salehzadeh M, Amiri M, Fathinasab M (2018) A literature review of asphaltene entity, precipitation and deposition: introducing recent models of deposition in the well column. *J Oil Gas Petrochem Sci* 1(3):83–89
- Zendehboudi S, Ahmadi MA, Mohammadzadeh O, Bahadori A, Chatzis I (2013) Thermodynamic investigation of asphaltene precipitation during primary oil production: laboratory and smart technique. *Ind Eng Chem Res* 52(17):6009–6031
- Zendehboudi S, Shafiei A, Bahadori AR, James LA, Elkamel A, Lohi A (2014) Asphaltene precipitation and deposition in oil reservoirs—technical aspects, experimental and hybrid neural network predictive tools. *Chem Eng Res Des* 92:857–875

**Publisher's Note** Springer Nature remains neutral with regard to jurisdictional claims in published maps and institutional affiliations.